UNIVERSITAT ROVIRA i VIRGILI

STUDIES ON THE INFLUENCE OF IONIC LIQUIDS ON THE SYNTHESIS OF $Cu_2(OH)PO_4$ AND TiO_2 CATALYSTS

David Gaya Tornos

Directed by: Dr M. Elena Fernández Gutiérrez

June 2019

Declaration of originality

I am responsible for the work submitted in this project. The original work is my own, except as specified in the acknowledgments and in the references, and neither the project nor the original work contained therein has been previously submitted to any institution for the award of a degree.

David Gaya Tornos, 5 June 2019

Abstract

The growing importance of TiO_2 for its interesting properties as a photocatalysts has raised a lot of efforts to overcome one of its main disadvantages: its wide bandgap limits light absorption to the UV region. Hence, photocatalytic activity is highly limited.

New composite materials with good light absorbing and photocatalytic properties stand as a good choice to overcome this barrier. $Cu_2(OH)PO_4$ is a good IR-absorbing material with reportedly good photo-oxidation properties. Thus, composites of TiO_2 and $Cu_2(OH)PO_4$ could become very interesting for new heterogeneous catalysis.

In this research work, the separate growth of $Cu_2(OH)PO_4$ and TiO_2 is studied under the influence of different ionic liquids (ILs) and other conditions, aiming to synthesize nanoparticles of both compounds. Usage of $[Amim]H_2PO_4$ seems to be a very promising route to prepare TiO_2 and $Cu_2(OH)PO_4$ particles in the desired size for further application as photocatalysts.

Materials were characterised using XRD, IR spectroscopy and SEM.

INDEX

1. INTRODUCTION

1.1. Theoretical background

TiO_2 has widely been used as photocatalyst because of its ability to convert photons into chemical energy, derived from its properties as a semiconductor, and oxidize organic pollutants. It is a non-toxic, corrosion-resistant, environmentally-friendly and highly photo-chemically stable material. All these characteristics, plus being a very simple material, make TiO_2 a very convenient material for the manufacture of catalysts.[1,2] Despite all of its advantages, the bandgap for titania (common name for TiO_2) is 3.0-3.2 eV, which highly limits its catalytic performance to the UV region of the electromagnetic spectrum.[1,3–5] This limitations led to develop new materials able to perform catalytic activity under a wider range of light conditions.

The UV-absorption properties of TiO_2 have been applied for over a hundred years in chemistry, medicine and industry.[6] Maybe the most known example among these applications is the usage of TiO_2 in sunscreens.[3] As UV light is absorbed, the skin is protected from this harmful radiation that might cause melanoma and other skin tumours.[7] Its oxidizing nature is applied in self-cleaning materials with anti-microbial properties in coatings for hospital touch-surfaces.[4] Other applications range from research on the sustainable production of H_2 to water-treatment processes (oxidation of organic compounds and reduction of heavy metals).[2]

According to IUPAC, a semiconductor is a material "whose conductivity, due to charges of both signs, is normally in the range between that of metals and insulators and in which the electric charge carrier density can be changed by external means".[8] Conductivity in such materials is due to the promotion of electrons from the compound's valence band to the conduction band after the absorption of energy. Bands are separated from one another by an energy gap known as bandgap. The width of this gap sets the operating conditions on which the semiconductor can work because low-energy conditions (such as low temperature or darkness) will not allow valence electrons to promote.

In the case of a photocatalyst, when photons collide with the material, electrons promote from the valence band to the conduction band, thus generating a positive charge (a "hole") in the former. Both electrons and holes are charge carriers and can move inside the crystal, both taking part in the photocatalytic process.

Eventually, the electrons and holes reach the surface of the particle and oxidize or reduce, respectively, chemical species adsorbed there. In titania, these chemical species are usually surface water or atmospheric oxygen, which reduce to reactive oxygen species (ROS). It is these

ROS that catalyse the redox main reactions (*e.g.* oxidation of organic water pollutants). Another phenomenon involving electrons and holes is recombination, which nullifies the photocatalytic activity. This later process occurs in crystal defects and grain boundaries.

Thus, it is of great importance to synthesize particles as small and crystalline as possible to effectively increase the number of charge carriers that end up producing ROS and avoid recombination.

Figure 1 shows the splitting of water in a titania particle as an example of this mechanism.[2]

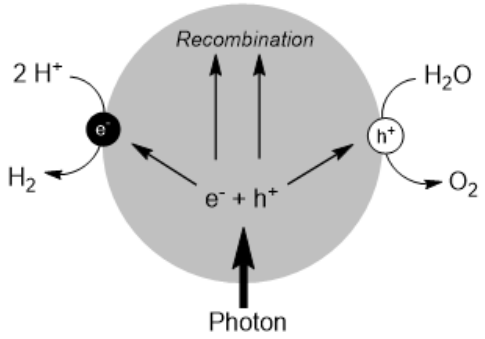

Figure 1. Splitting of water in a TiO_2-photocatalysed system.

As mentioned before, the big bandgap of titania is the main disadvantage of its usage as a photocatalyst, because it would only work under UV light. To overcome this disadvantage, doped TiO_2 and composite materials have been lately prepared and proved to be quite efficient.[1,2,4,5]

Libethenite (common name for $Cu_2(OH)PO_4$) is also a semiconductor that absorbs light in the IR and visible regions of the light spectrum. By mixing this two compounds it was expected to enhance the photocatalytic activity of titania. Therefore, $Cu_2(OH)PO_4$ and TiO_2 composite materials were aimed to be prepared.

Some literature can be found concerning libethenite, and its application as a photocatalyst have already been studied.[9–12] Libethenite presents itself as a good photocatalyst by two main reasons: it has 50% penta-coordinate Cu atoms, which are known to be highly active catalytical sites, and hydroxyl groups which improve photocatalytic activity by forming hydroxyl radicals and other important intermediates in the catalytical process.[10,12] However, there is no literature about the preparation of TiO_2-$Cu_2(OH)PO_4$ materials. Thus, it was thought it would be very interesting to investigate this rather unexplored field.

1.2. Aim of the project

The main aim of this investigation is to synthesize libethenite and titania nanoparticles to be used later on the preparation of TiO_2-$Cu_2(OH)PO_4$ composite materials. This includes the study of the influence of different ILs in the size and the morphology of $Cu_2(OH)PO_4$ and TiO_2 particles.

2. EXPERIMENTAL

All the processes, reactions and characterisation, as well as the bibliographic work, have been carried out in the ISTeC facility of the Nottingham Trent University, Clifton Campus[a]. Work has kindly been supervised by Dr Valeria Puddu as part of her research in novel TiO_2-based photocatalysts.

2.1. Chemicals

All chemicals were used as commercially provided from Sigma Aldrich, without further purification. [bmim]Cl was purchased from Fluorochem.

Table 1. List of reagents with the respective hazard pictograms and handling recommendations.

Formula or name	Pictograms	Manipulation and storage recommendations
$Cu(NO_3)_2 \cdot 3H_2O$, ≤99% wt.		Laboratory coat, safety goggles and gloves must be worn. Keep in a fresh, well-aired place, inside a hermetically closed container
$Ti(BuO)_4$, 97% wt.		Laboratory coat, safety goggles and gloves must be worn. Keep in a fresh, well-aired place, inside a hermetically closed container.
Hexylamine, 99% wt.		Laboratory coat, safety goggles and gloves must be worn. Keep in a fresh, well-aired place, inside a hermetically closed container.
1-Butyl-3-methylimidazolium chloride ([bmim]Cl), ≤98% wt.		Laboratory coat, safety goggles and gloves must be worn. Avoid contact with skin. Storage at moderate temperature in dry, well-ventilated environments Avoid washing into water courses.
$NH_4H_2PO_4$, ≤98% wt.	-	Laboratory coat and safety goggles must be worn.

[a] Clifton Lane, Clifton, Nottingham (United Kingdom) NG11 8SN.

Na_2HPO_4	-	Laboratory coat and safety goggles must be worn.
H_3PO_4, 85% wt.		Laboratory coat, safety goggles and nitrile gloves must be worn.
1-Benzyl-3-methylimidazolium chloride ([Bnmim]Cl), ≤97% wt.		Laboratory coat, safety goggles and gloves must be worn
1-Allyl-3-methylimidazolium chloride ([Amim]Cl), ≤97% wt.		Laboratory coat, safety goggles and gloves must be worn
1-Decyl-3-methylimidazolium chloride ([C10mim]Cl), ≤96% wt.		Laboratory coat, safety goggles and gloves must be worn
NH_3 solution, 34% wt.		Laboratory coat, safety goggles and gloves must be worn. Keep in a fresh, well-aired place, inside a hermetically closed container.
NaOH pellets		Laboratory coat, safety goggles and gloves must be worn. Keep in a fresh place inside a hermetically closed container.

2.1. Synthesis of libethenite nanoparticles

$Cu_2(OH)PO_4$ nanoparticles were chosen as the target product in this research work. Later preparation of TiO_2-$Cu_2(OH)PO_4$ composite materials would start from that point. Besides the catalytic advantages of nanoparticles, from the practical point of view it is also easier to homogeneously mix smaller particles of two different solids if they are small. Hence, the methodologies presented in this section aim to produce libethenite nanoparticles.

First, bibliographic work had to be done to find preparation methods for libethenite nanoparticles. Three were found: precipitation,[10] hydrothermal[9,11,13] and ionic liquid-assisted

hydrothermal.[12] All of them were carried out following the instructions from literature and using $Cu(NO_3)_2{\cdot}3H_2O$ as a starting material.

2.1.1. Precipitation method

$Cu(NO_3)_2{\cdot}3H_2O$ and $NH_4H_2PO_4$ (molar ratio of 2:1) were separately dissolved in water. These solutions were subsequently mixed and stirred together for 24 h at 60 °C. pH was adjusted to 7 with commercial NH_3 (30% wt.). Afterwards, the precipitate was filtered and washed with water, then dried in a vacuum oven overnight at 80 °C.[10] Sample was named Lib_blue.

2.1.2. Hydrothermal method

$Cu(NO_3)_2{\cdot}3H_2O$ and Na_2HPO_4 were dissolved in water, adjusting pH to 7 with a NaOH solution. The mixture was poured into a 45 mL Teflon-lined stainless-steel autoclave and heated up to 180 °C for 24 h. Afterwards, a green precipitate was recovered by filtration and dried in a vacuum oven overnight at 80 °C.

Not all the precursor mixture fitted in the autoclave, so it was split in two; the second fraction was poured into the autoclave almost 30h after it was prepared. Respective samples were called Lib_Hyd1 and Lib_Hyd2.

2.1.3. IL-assisted hydrothermal method

The chosen ionic liquid (IL) was 1-butyl-3-methylimidazolium dihydrogen phosphate, $[bmim]H_2PO_4$, which acted both as a crystal-size controller and as a $H_2PO_4^-$ donor. Synthesis and characterization of this IL was necessarily carried out in the laboratory as described in literature[14–16] because it is not widely available in the market.

$Cu(NO_3)_2{\cdot}3H_2O$ and 1mL hexylamine were dissolved in water. $[bmim]H_2PO_4$ was added in a $Cu(NO_3)_2{\cdot}3H_2O$:IL molar ratio of 1:4. The mixture was stirred for 10 min and poured into a 45 mL Teflon-lined stainless-steel autoclave and heated up to 180 °C for 24 h. A green precipitate was recovered by filtration and was dried overnight in a vacuum oven at 80 °C. Sample was named Lib_IL.

2.1.4. Alternatives for the IL-assisted method

Because of the failure at synthesizing $Cu_2(OH)PO_4$ nanoparticles by the IL-assisted method, experimental errors were suspected, and the method was tried again. Some conditions were changed to check if they had an influence in the morphology and the size of the particles. Three samples were obtained: L1, LA and LB. Table 2 summarizes the way these samples were prepared.

Table 2. Preparation method for every sample in the testing of the IL-assisted method. Drying was carried out at room temperature and atmospheric pressure.

Sample name	Preparation method
L1	1) Dissolve 2 mmol $Cu(NO_3)_2*3H_2O$ in 24 mL water. 2) Add 1 mL hexylamine. 3) Add 4 mmol IL. *Autoclave: 24 h, 180 °C. Then filter and dry.*
LA	1) Dissolve 1 mL hexylamine in 24 mL water 2) Add 2 mmol $Cu(NO_3)_2*3H_2O$. 3) Add 4 mmol IL. *Autoclave: 24 h, 180 °C. Then filter and dry.*
LB	1) Dissolve 2 mmol $Cu(NO_3)_2*3H_2O$ in 24 mL water 2) Add 1 mL hexylamine 3) Add 8 mmol IL *Autoclave: 24 h, 180 °C. Then filter and dry.*

2.1.5. Synthesis of $Cu_2(OH)PO_4$ particles with various ILs

Preparation of 3 samples (L2, L3 and L4) of libethenite was carried out in the same fashion as sample L1 (Table 2), though the IL was different in each one. Different side chain sizes and characteristics were tried. Table 3 and Figure 2 sum up the nature of these side chains (R) and match each IL with a sample.

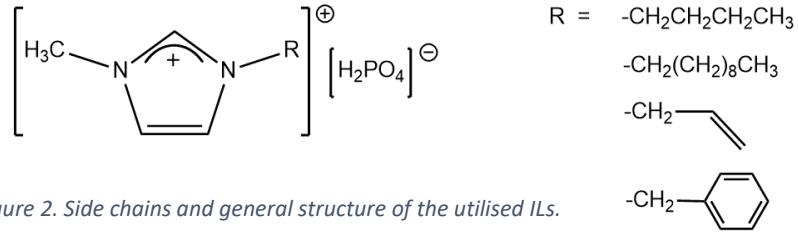

Figure 2. Side chains and general structure of the utilised ILs.

Table 3. Sample names and respective ILs. Sample L0 is the same as Lib_Hyd1 from section 2.1.2, but its name was shortened before this section of the project began to make writing and reading easier.

Sample name	R	Ionic liquid
L0	No IL was used	No IL was used
L1	Butyl	$[bmim]H_2PO_4$
L2	Decyl	$[C10mim]H_2PO_4$

L3	Allyl	$[Amim]H_2PO_4$
L4	Benzyl	$[Bnmim]H_2PO_4$

As in the case of $[bmim]H_2PO_4$ synthesis of ILs was necessarily carried out in the laboratory because the phosphate ILs are not usually commercially available. Yields were always above 90%.

In a typical synthesis, 50 mmol of the chloride IL is dissolved in 75 mL of CH_2Cl_2 followed by the dropwise addition of equimolar H_3PO_4. After stirring for 24 h, solvent is removed by rotary evaporation. Along with CH_2Cl_2, also HCl by-product is removed.

Preparation of $[C10mim]H_2PO_4$ was slightly more complicated because the final product was a waxy substance and rotary evaporation could not be conducted. Instead, the product was dissolved in 15mL of chloroform with stirring and heating (50 °C). After a light brown solution formed, solvent was removed by rotary evaporation and a dense, viscous, amber-coloured product was obtained.

2.2. Synthesis of TiO_2 particles with various ILs

IL-assisted synthesis of TiO_2 particles was carried out as described by literature.[17,18] $Ti(BuO)_4$, ethanol and chloride IL (different for each sample, see Table 4) were mixed in a molar ratio of 10:50:2 and stirred together for 24 h. Then the mixture is refluxed at 92 °C. After 1h, water is added dropwise in a molar ratio $Ti(BuO)_4$:H_2O of 1:8. The mixture is subsequently refluxed again for 3 h at 92 °C.

A white precipitate formed. It was collected by filtration and washed with acetone and ethylic ether. Then it was dried at atmospheric pressure and room temperature. After drying, samples were calcined at 600 °C for 3 h. Sample T0 was divided in three: T0a, T0b and T0c. These were calcined at temperatures of 500, 550 and 600 °C respectively. The aim of this experiment was to study the influence of calcination temperature on the structure of as-prepared and calcined TiO_2 particles.

Table 4. Titania samples and ILs utilised in their preparation.

Sample name	**Ionic liquid**
T0	No IL was used

T1	[bmim]Cl
T2	[C10mim]Cl
T3	[Amim]Cl
T4	[Bnmim]Cl

2.3. Characterisation

The morphology of the TiO_2 and $Cu_2(OH)PO_4$ was determined by SEM (JEOL JSM-7100F in secondary electron mode with accelerating voltages from 5 to 20 kV). Samples were attached to aluminium stubs using double-sided carbon adhesive tape. 10 nm of gold coating was required for TiO_2 samples.

Identification of solids (*i.e.* titania and libethenite) was carried out via XRD (PANalytical X'Pert PRO, Cu Kα radiation with a wavelength of 1.54056 Å), which was also used to check the crystallinity of samples. Solids were packed into aluminium sample holders and scanned from 5° to 90° of 2θ at an accelerating voltage of 45 kV and a filament current of 40 mA. Besides, $Cu_2(OH)PO_4$ samples and dihydrogen ILs were also identified by IR spectroscopy (Agilent Cary 360 FTIR).

3. RESULTS

3.1. Precipitation, Hydrothermal and IL-assisted methods

The products of these methods were characterised by XRD, SEM and UV-visible and IR spectroscopy (see APPENDIX 1 for spectroscopic and XRD data). Results showed that, despite libethenite was successfully synthesized in the hydrothermal and IL-assisted method, the particles were not in the nanoscale but much bigger (about 15µm). In the precipitation method, though, much of the precursor did not react. Hence, Lib_blue was contaminated with it and the yield was not very high.

The experiment with the IL suggested that the size of the aliphatic substituents of the IL had an influence in the growth of the libethenite crystals. In consequence, experiments with imidazole-based ILs with different sizes could be tried. Bulkier ILs are supposed to interfere in the formation of crystals as steric hinderance prevents libethenite and titania particles to grow big.

3.1.1. Alternatives for the IL-assisted method

IR spectroscopy (check APPENDIX 3 for spectra) and XRD allowed to successfully characterize L1, LA and LB as crystalline $Cu_2(OH)PO_4$ (orthorhombic system and Pnnm space group, see $Cu_2(OH)PO_4$ JCDD file) with no noticeable differences in crystallinity between samples. SEM pictures of the three samples revealed interesting differences between them, concerning both the morphology and the size of the particles.

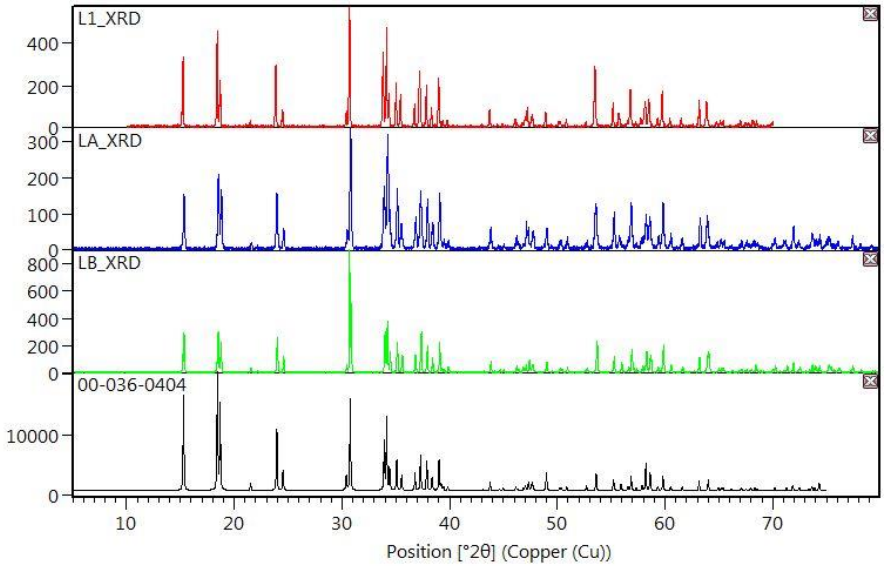

Figure 3. Diffractograms for samples L1, LA, LB and a simulation for the JCDD pattern of orthorhombic libethenite.

Comparison of SEM pictures of samples L1 and LA (Figure 5) demonstrated that the order of addition of reagents has an influence on the morphology of the growing $Cu_2(OH)PO_4$ particles. While particles L1 maintained a truncated bipyramidal shape (Figure 4), LA particles were not homogeneously shaped and showed lots of different morphologies.

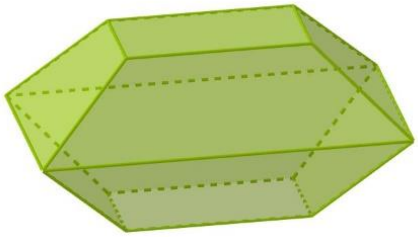

Figure 4. Schematic representation of the shape of L1 particles made with GeoGebra Classic 5 (GeoGebra - Dynamic Mathematics for Everyone www.geogebra.org).

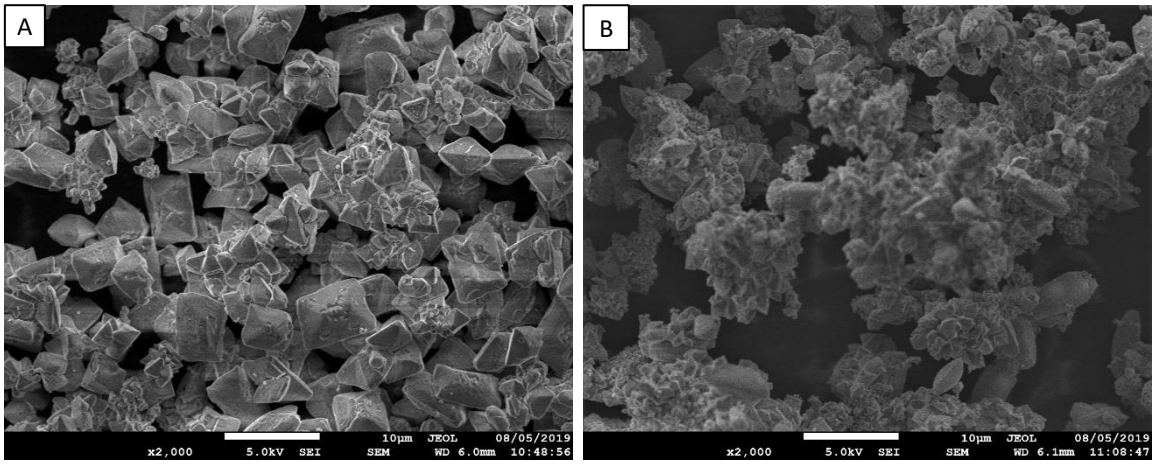

Figure 5. SEM pictures of samples at a magnification of x2000. A) L1; B) LA.

The amount of IL used in the synthesis had a strong influence in the growth of crystals. The presence of IL was thought to prevent crystals to grow big because of its steric hinderance. However, results showed that bigger amounts of IL yielded much bigger crystals with a slightly different morphology: instead of being truncated bipyramids, LB particles were squared elongated bipyramids.

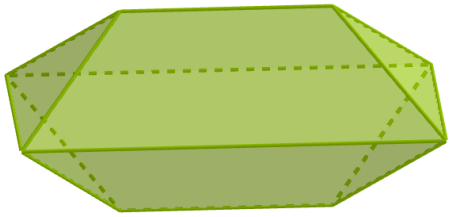

Figure 6. Schematic representation of LB bipyramids also made with GeoGebra Classic 5.

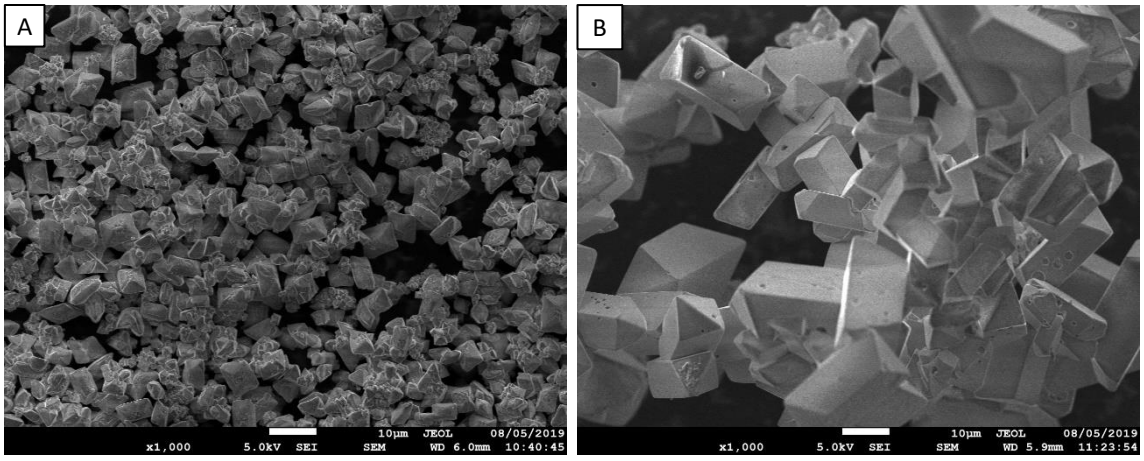

Figure 7. SEM pictures at a magnification of x1000. A) L1; B) LB.

3.2. Synthesis of $Cu_2(OH)PO_4$ particles using various ILs

Samples were successfully synthesized and characterized as $Cu_2(OH)PO_4$ by IR spectroscopy (see APPENDIX 3) XRD and SEM. Products matched with JCDD pattern 36-0404 corresponding to orthorhombic libethenite crystals and Pnnm space group.

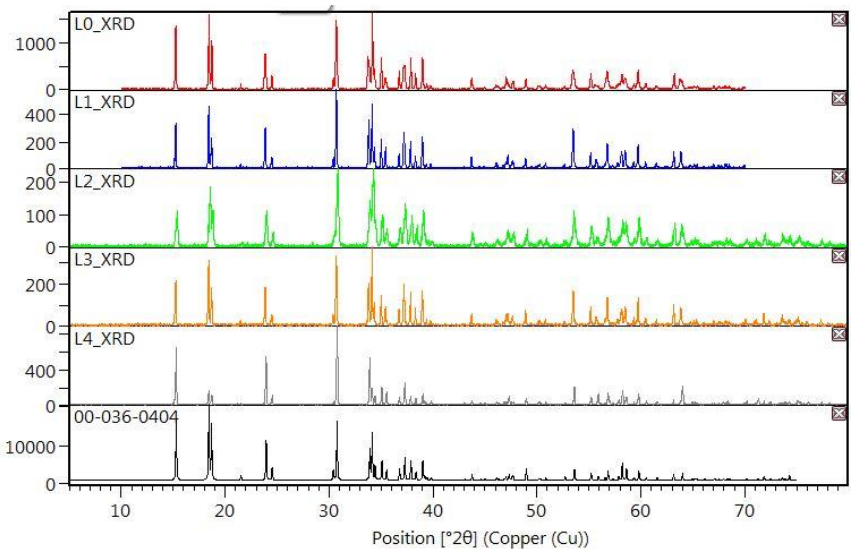

Figure 8. Diffractograms of the different libethenite samples and a reference pattern simulation (see $Cu_2(OH)PO_4$ JCDD file).

SEM pictures showed big differences between samples prepared with different ILs. In general, the usage of ILs provoked an increase in the particle size in comparison with the non-IL reference (L0). Besides, bulkier ILs yielded bigger particles without a clear bipyramidal shape. Smaller ILs gave smaller crystals with better defined morphology.

The IL that gave smaller particles was 1-allyl-3-methylimidazolium dihydrogen phosphate ([Amim]H_2PO_4). These particles were in the nanoscale and had a quite homogeneous morphology.

Results also revealed that π systems conjugated with the imidazole ring, did not have a clear influence in the morphology nor the size of the particles.

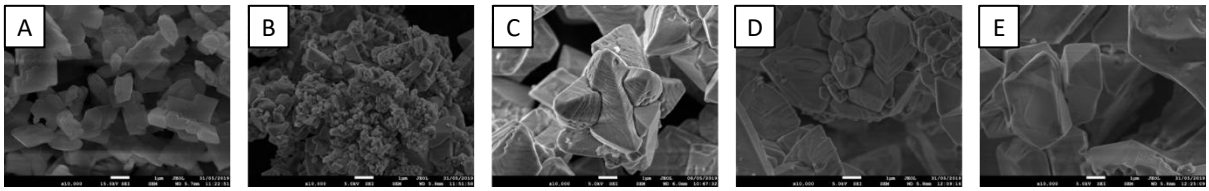

Figure 9. SEM pictures of libethenite samples. From A to E the size of the R chain of the utilised IL increases as well as the size of particles. A) L0; B) L2; C) L1; D) L3; E) L4

3.3. Synthesis of TiO_2 particles with various ILs

3.3.1. Influence of the calcination temperature

The study on the influence of calcination temperature in the growth of TiO_2 did not reveal any significative difference between calcination at 500, 550 or 600°C. XRD data allowed to characterize samples T0a, T0b and T0c as anatase (see TiO2 (anatase) JCDD file). Only crystallinity seems to be affected by calcination temperature because diffraction peaks from sample T0a are slightly broader than those from T0b and T0c, but these differences are not regarded as important.

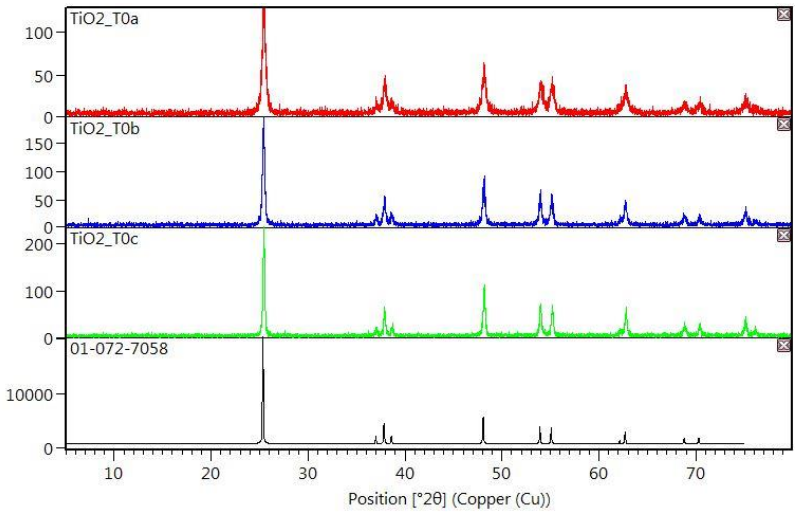

Figure 10. Diffractograms for samples T0a, T0b, T0c and a simulation of anatase JCDD pattern.

SEM pictures did not reveal any important differences between samples T0a, T0b and T0c.

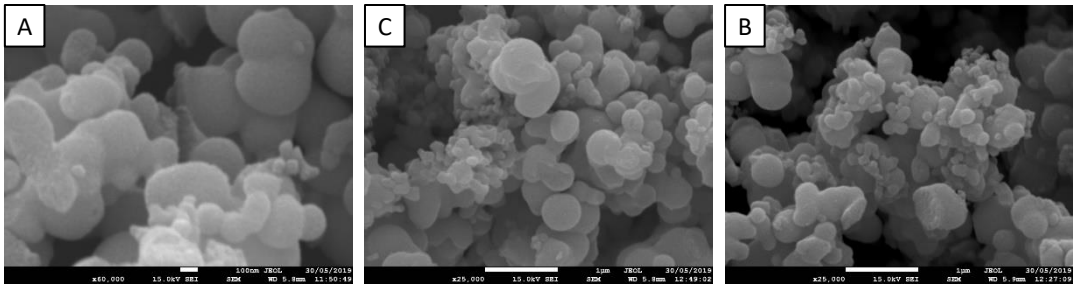

Figure 11. SEM pictures at x25000 magnification of: A) T0a, B) T0b and C) T0c.

3.3.2. TiO_2 samples prepared with different ILs

XRD characterisation of IL-prepared titania showed that in some cases the samples did not contain a single phase of TiO_2, but two. This is especially important in T3 and T4, which are a mixture of anatase and rutile (go to APPENDIX 2 and Table 4 for more information). The other samples had smaller amounts of rutile and consisted mainly of anatase.

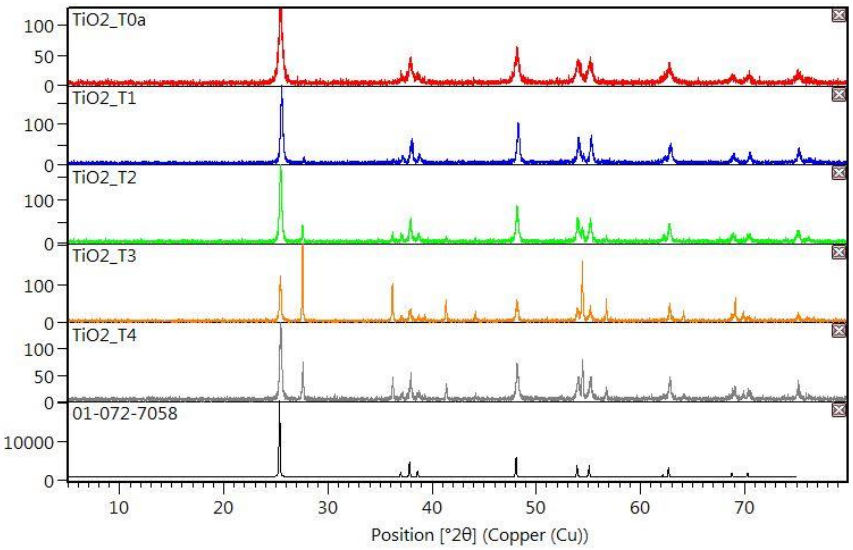

Figure 12. Diffractograms for samples T0a, T1, T2, T3, T4 and a simulation for anatase JCDD diffraction pattern.

SEM pictures revealed particles as T0a, T1 and T4 crystals were quite the same size and morphology despite T0a was not synthesized with an IL and the alkyl R substituents in the imidazolium rings of T1 and T4 had very different lengths. On the contrary, T2 and T3 particles (which were prepared using ILs with conjugated imidazolium rings) were much smaller. Thus, the presence of π systems with delocalized charges causes a decrease of the general particle size, whereas the size of alkyl substituents does not have a noticeable influence on the growth of TiO_2 crystals. As suggested by literature for libethenite,[12] this could be due to a stabilization of the growing facets by the ILs. Thus, the system tends to grow the existing nuclei rather than creating new crystals.

However, regarding the XRD data, the size of substituents (conjugated or not) does have an influence on the growing crystallographic phase of TiO_2. XRD for T3 and T4 (the ones prepared with bulkier ILs) shows an increasing amount of rutile in addition of anatase, a phenomenon less significative in other titania samples.

4. CONCLUSIONS

Comparison between samples demonstrated that ILs with short side chains have the desired effect on the synthesis of nanoparticles. When such structures become bulkier, crystals grow bigger. This result is consistent with the IL-method testing: bulkier ILs or bigger amounts of ILs yield bulkier crystals do not affect noticeably in the growth of libethenite particles.

The presence of conjugated imidazolium rings does not seem to have a clear influence on the size of the particles nor their morphology. Despite the presence of different ILs (conjugated or aliphatic) does not have a clear influence on the morphology of particles, it does on their size.

Regarding the objective of the project, which was to synthesize nanoparticles of $Cu_2(OH)PO_4$, the usage of $[Amim]H_2PO_4$ stands as the best choice for an IL-assisted method for libethenite preparation. Besides, precursor [Amim]Cl was easy to work with, while other ILs such as [C10mim]Cl were very dense and viscous, and manipulation was more difficult. Also, synthesis of the phosphate IL was simple and gave good yields.

Concerning TiO_2, SEM pictures demonstrated that the presence of conjugated imidazolium rings (from [Amim]Cl and [Bnmim]Cl) yields smaller particles than ILs with alkyl side chains. [bmim]Cl and [C10mim]Cl do not have a substantial influence on the growth of titania, as samples T1 and T4 were very similar to those prepared without ILs (T0a, T0b and T0c).

All these reasons make the usage of $[Amim]H_2PO_4$ a very promising strategy for the preparation of $Cu_2(OH)PO_4$ and TiO2 with the desired particle size, which makes it a good starting point for the synthesis of TiO_2-$Cu_2(OH)PO_4$ composite photocatalysts.

Acknowledgements

In the first place, I would like to thank my supervisor, Dr Valeria Puddu, for her consistent support and helpful guidance throughout the project which have been essential for the completion of this research work. It has been extremely eye-opening for me being part of this project and developing my own research.

In the second place, I would like to heartily thank Dr Anna Solà Rabadà for her valuable advice and the most resourceful conversations we have had during my stay at Nottingham Trent University. Also, I would like to thank the technical staff in Clifton Campus for their patience and good attention I received.

In the third place, I would like to acknowledge the Universitat Rovira i Virgili and the European Union, especially the Erasmus+ projects, for rendering me the opportunity to develop this research project abroad both economically and institutionally.

Finally, I would like to warmly thank my family and friends for their support, trust and always believing in me and my project.

5. REFERENCES

(1) Tang, Q.; Meng, X.; Wang, Z.; Zhou, J.; Tang, H. One-Step Electrospinning Synthesis of TiO 2 /g-C 3 N 4 Nanofibers with Enhanced Photocatalytic Properties. *Appl. Surf. Sci.* **2018**, *430*, 253–262.

(2) Kudo, A.; Miseki, Y. Heterogeneous Photocatalyst Materials for Water Splitting. *Chem. Soc. Rev.* **2009**, No. 1, 253–260.

(3) Hofmann, S.; Wang, J. Y.; Zalar, A. Backscattering Effect in Quantitative AES Sputter Depth Profiling of Multilayers Approach to the Local Backscattering Factor in Sputter. *Surf. Interface Anal.* **2006**, *38* (August), 473–477.

(4) Krumdieck, S. P.; Boichot, R.; Gorthy, R.; Land, J. G.; Lay, S.; Gardecka, A. J.; Polson, M. I. J.; Wasa, A.; Aitken, J. E.; Heinemann, J. A.; et al. Nanostructured TiO 2 Anatase-Rutile-Carbon Solid Coating with Visible Light Antimicrobial Activity. *Sci. Rep.* **2019**, *9* (1), 1–11.

(5) Kato, K.; Xin, Y.; Shirai, T. Structural-Controlled Synthesis of Highly Efficient Visible Light TiO2 Photocatalyst via One-Step Single-Mode Microwave Assisted Reaction. *Sci. Rep.* **2019**, *9* (1), 4900.

(6) Chen, X.; Mao, S. S. Titanium Dioxide Nanomaterials: Synthesis, Properties, Modifications, and Applications. **2007**.

(7) WHO | Health Effects of UV Radiation. *WHO* **2017**.

(8) Semiconductor. In *IUPAC Compendium of Chemical Terminology*; IUPAC: Research Triagle Park, NC.

(9) Roumila, Y.; Abdmeziem, K.; Rekhila, G.; Trari, M. Semiconducting Properties of Hydrothermally Synthesized Libethenite Application to Orange G Photodegradation. *Mater. Sci. Semicond. Process.* **2016**, *41*, 470–479.

(10) Pérez-Barrado, E.; Darton, R. J.; Guhl, D. Synthesis and Applications of Near-Infrared Absorbing Additive Copper Hydroxyphosphate. *MRS Commun.* **2019**, No. 2018, 1070–1078.

(11) Chen, C.; Zhou, Y.; Wang, N.; Cheng, L.; Ding, H. Cu2(OH)PO4/g-C3N4 Composite as an Efficient Visible Light-Activated Photo-Fenton Photocatalyst. *RSC Adv.* **2015**, *5* (116), 95523–95531.

(12) Duan, X.; Xiao, S.; Liu, Y.; Huang, H.; Wang, D. Ionic Liquid-Assisted Fabrication of Copper Hydroxyphosphate Nanocrystals with Exposed {100} Facets for Enhanced Photocatalytic Activity. *Nanotechnology* **2015**, *26*.

(13) Wang, G.; Huang, B.; Ma, X.; Wang, Z.; Qin, X.; Zhang, X.; Dai, Y.; Whangbo, M. Cu2(OH)PO4, a Near-Infrared-Activated Photocatalyst. *Angew. Commun.* **2013**, *2*, 4810–4813.

(14) Wu, P.; Dai, B.; Chao, Y.; Wu, Y.; Jiang, W.; Li, C.; Zhu, W.; Li, H. Graphene-like Boron Nitride Anchored Brönsted Acid Ionic Liquids as Metal-Free Catalyst for Advanced Oxidation Process. *Mol. Catal.* **2017**, *436*, 53–59.

(15) Klähn, M.; Mathias, G.; Kötting, C.; Nonella, M.; Schlitter, J.; Gerwert, K.; Tavan, P. IR Spectra of Phosphate Ions in Aqueous Solution: Predictions of a DFT/MM Approach Compared with Observations. *J. Phys. Chem. A* **2004**, *108* (29), 6186–6194.

(16) Rivera-Rubero, S.; Baldelli, S. Surface Characterization of 1-Butyl-3-Methylimidazolium Br-, i-, PF6-, BF4-, (CF 3so2)2N-, SCN-, CH3so3-, CH3so4-, and (CN)2N- Ionic Liquids by Sum Frequency Generation. *J. Phys. Chem. B* **2006**, *110* (10), 4756–4765.

(17) Alammar, T.; Birkner, A.; Shekhah, O.; Mudring, A. V. Sonochemical Preparation of TiO2 Nanoparticles in the Ionic Liquid 1-(3-Hydroxypropyl)-3-Methylimidazolium-Bis(Trifluoromethylsulfonyl)Amide. *Mater. Chem. Phys.* **2010**, *120* (1), 109–113.

(18) Avellaneda, R. S.; Ivanova, S.; Sanz, O.; Romero-Sarria, F.; Centeno, M. A.; Odriozola, J. A. Ionic Liquid Templated TiO2 Nanoparticles as a Support in Gold Environmental Catalysis. *Appl. Catal. B Environ.* **2009**, *93* (1–2), 140–148.

APPENDIX 1

Display of several spectra that allowed the characterization of libethenite samples.

IR spectra of libethenites

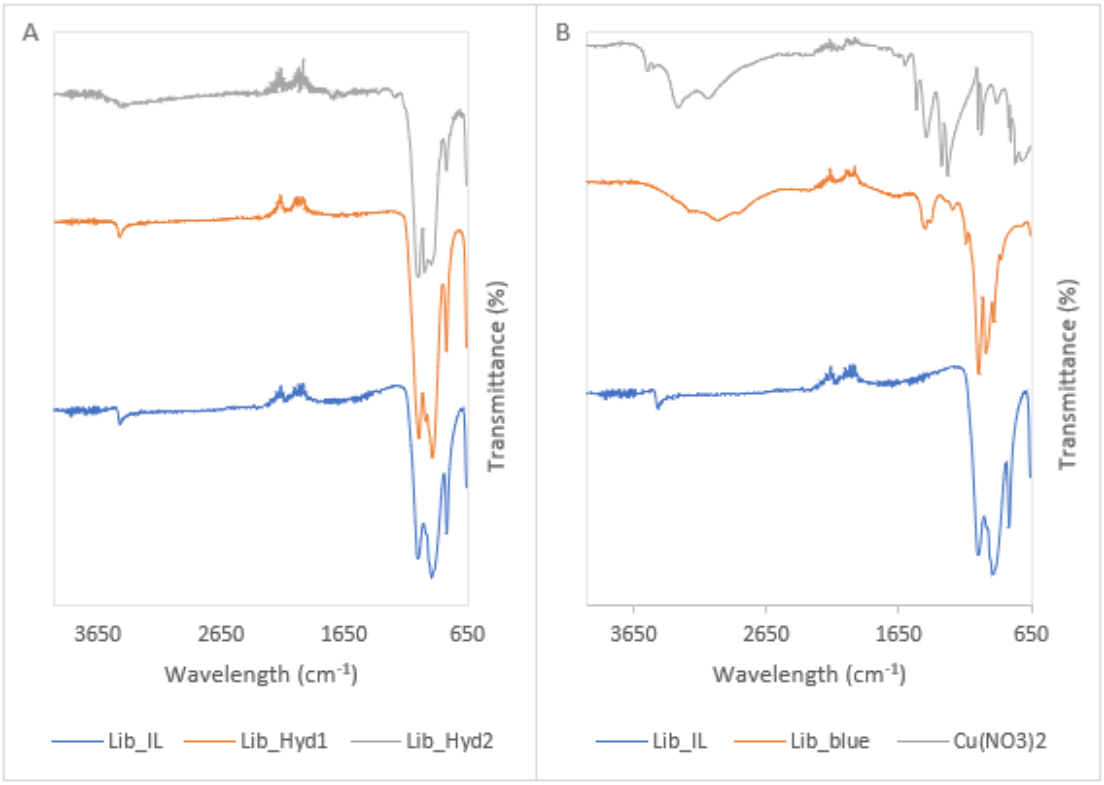

Figure 13. A) IR spectra for libethenite samples. B) IR spectra for Lib_blue, Lib_IL and commercial $Cu(NO_3)_2{\cdot}3H_2O$.

Figure 13.A shows that samples Lib_IL, Lib_Hyd1 and Lib_Hyd2 behave similarly and match one with each other and with literature.[11] Bands at *ca.* 3465 and 810cm^{-1} are assigned to the stretching and bending, respectively, of hydration water. Peaks at *ca.* 1040 and 930cm^{-1} are due to the asymmetric and symmetric stretching of phosphate ions.

As displayed in Figure 13.B, Lib_blue has a big amount of copper (II) nitrate trihydrate, which gives the blue colour that characterized this sample.

XRD data

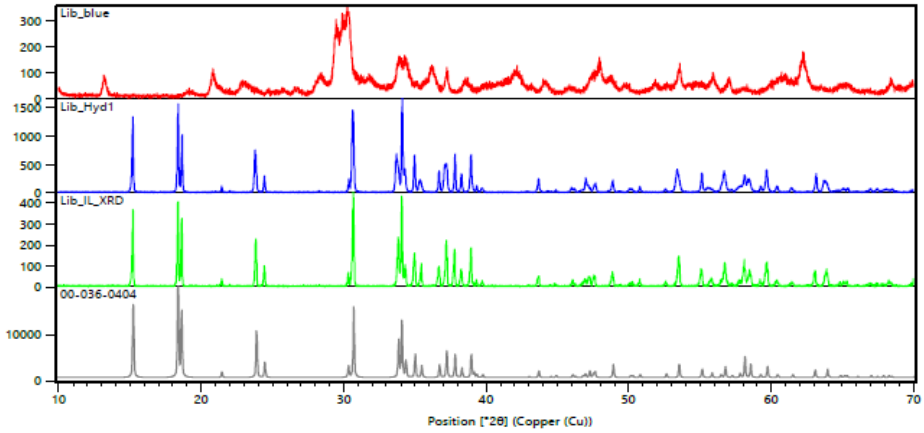

Figure 14. Diffractograms for Lib_blue, Lib_Hyd1, Lib_IL and a simulation of the JCDD file of libethenite.

XRD data demonstrate that samples Lib_Hyd1 and Lib_IL identify as highly crystalline orthorhombic $Cu_2(OH)PO_4$ in the Pnnm space group (see Cu2(OH)PO4 JCDD file), whereas Lib_blue is not.

UV-visible spectra

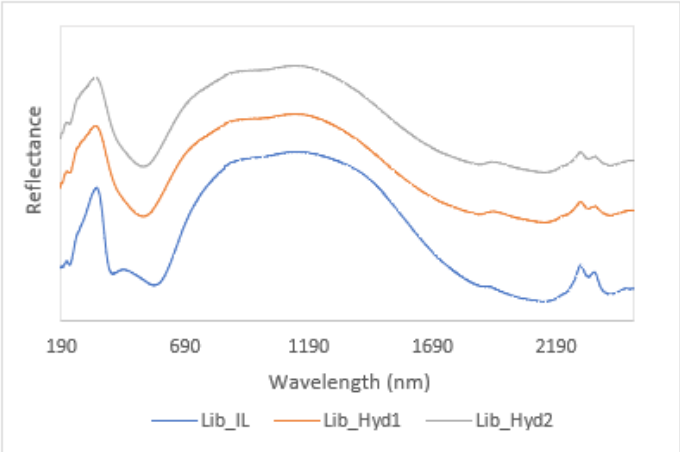

Figure 15.UV-visible spectra of Lib_IL, Lib_Hyd1 and Lib_Hyd2.

Figure 15 shows the UV spectra of libethenite samples. Lib_blue was not analysed because IR and XRD data already showed that the synthesis of the compound had not been successful.

As shown, libethenite is a compound with good absorption in the IR and near-IR region of the electromagnetic spectrum.

APPENDIX 2

JCDD files for the two studied compounds: $Cu_2(OH)PO_4$ and TiO_2 (anatase and rutile phases).

$Cu_2(OH)PO_4$ JCDD file

Name and formula

Reference code:	00-036-0404
Mineral name:	Libethenite
Compound name:	Copper Phosphate Hydroxide
PDF index name:	Copper Phosphate Hydroxide
Empirical formula:	Cu_2HO_5P
Chemical formula:	$Cu_{2+2}(PO_4)(OH)$
Mineral classification:	Andalusite (Group), phosphate (Subgroup)

Crystallographic parameters

Crystal system:	Orthorhombic
Space group:	Pnnm
Space group number:	58
a (Å):	8.0633
b (Å):	8.3981
c (Å):	5.8873
Alpha (°):	90.0000
Beta (°):	90.0000
Gamma (°):	90.0000
Calculated density (g/cm^3):	3.98
Measured density (g/cm^3):	3.97
Volume of cell (10^6 pm^3):	398.67
Z:	4.00
RIR::	-

Subfiles and quality

Subfiles:	Common Phase, Inorganic, Mineral, Mineral - Mineral, Mineral - Natural
Quality:	Star (S)

Comments

Color:	Green
Creation Date:	01/09/1986
Additional Patterns:	To replace 00-001-0274, 00-008-0107 and 00-033-0481. See PDF 01-072-0026, 01-072-0592 and 01-083-2264
Analysis:	Chemical analysis (wt.%): CuO 66.29, "P2 O5" 26.46, "As2 O5" 2.30, "H2 O" 4.04 Dana`s System of Mineralogy, 7th Ed., II 863 (1951). X-ray emission analysis: Cu, P, minor Fe, As. Color: Green. Sample Source or Locality: Specimen from Libethen, Neusohl, Czechoslovakia.

References

Primary reference: Blanchard, F., Dept. of Geology, University of Florida, Gainesville, Florida, USA., *ICDD Grant-in-Aid*, (1985)

Optical data: *Dana's System of Mineralogy, 7th Ed.*, **II**, 863, (1951)

Peak list

No.	h	k	l	d [Å]	2θ [°]	I [%]
1	1	1	0	5.80700	15.246	80.0

2	0	1	1	4.82000	18.392	100.0
3	1	0	1	4.75600	18.642	70.0
4	1	1	1	4.13600	21.467	6.0
5	1	2	0	3.72000	23.901	50.0
6	2	1	0	3.63300	24.482	16.0
7	0	0	2	2.94200	30.357	12.0
8	2	2	0	2.90800	30.721	75.0
9	1	3	0	2.64400	33.876	40.0
10	1	1	2	2.62700	34.102	60.0
11	2	2	1	2.60600	34.385	18.0
12	3	1	0	2.55900	35.037	25.0
13	0	3	1	2.52700	35.496	13.0
14	3	0	1	2.44400	36.743	14.0
15	1	3	1	2.41200	37.249	30.0
16	2	0	2	2.37600	37.834	25.0
17	3	1	1	2.34700	38.320	10.0
18	1	2	2	2.30900	38.976	25.0
19	2	3	0	2.29800	39.170	5.0
20	2	1	2	2.28700	39.366	3.0
21	3	2	0	2.26400	39.783	3.0
22	0	4	0	2.10000	43.038	1.0
23	2	2	2	2.06900	43.716	7.0
24	1	4	0	2.03100	44.577	1.0
25	4	0	0	2.01550	44.939	2.0
26	1	3	2	1.96740	46.100	3.0
27	4	1	0	1.95960	46.294	1.0
28	3	3	0	1.93900	46.815	2.0
29	3	1	2	1.93240	46.984	4.0
30	1	4	1	1.92080	47.285	7.0
31	0	1	3	1.91100	47.543	4.0
32	1	0	3	1.90650	47.662	6.0
33	1	1	3	1.85960	48.941	7.0
34	4	1	1	1.85960	48.941	7.0
35	4	2	0	1.81710	50.164	2.0
36	2	3	2	1.81170	50.324	2.0
37	3	2	2	1.79500	50.825	3.0
38	1	2	3	1.73620	52.676	2.0
39	4	2	1	1.73620	52.676	2.0
40	0	4	2	1.70950	53.564	14.0
41	4	0	2	1.66320	55.180	9.0
42	1	5	0	1.64410	55.877	5.0
43	2	2	3	1.62710	56.513	3.0
44	3	3	2	1.61930	56.810	12.0
45	0	3	3	1.60690	57.288	2.0
46	3	4	1	1.59290	57.839	4.0
47	5	1	0	1.58440	58.179	11.0
48	3	0	3	1.58440	58.179	11.0
49	2	4	2	1.57450	58.581	7.0
50	1	3	3	1.57450	58.581	7.0
51	3	1	3	1.55740	59.288	3.0
52	4	2	2	1.54610	59.765	12.0
53	5	1	1	1.52960	60.476	3.0
54	5	2	0	1.50550	61.548	3.0
55	0	0	4	1.47190	63.113	8.0
56	4	4	0	1.45400	63.981	9.0
57	1	5	2	1.43560	64.901	2.0
58	4	3	2	1.43010	65.181	2.0
59	1	1	4	1.42700	65.340	2.0
60	4	4	1	1.41200	66.123	1.0
61	5	1	2	1.39480	67.045	2.0
62	4	1	3	1.38680	67.484	1.0
63	1	6	0	1.37920	67.906	1.0
64	3	3	3	1.37920	67.906	1.0
65	2	5	2	1.37220	68.300	2.0
66	1	2	4	1.36860	68.504	1.0
67	5	2	2	1.34030	70.160	2.0
68	2	6	0	1.32240	71.253	2.0
69	2	2	4	1.31330	71.823	4.0
70	4	4	2	1.30400	72.416	2.0
71	4	5	0	1.29070	73.283	1.0
72	1	3	4	1.28610	73.588	3.0
73	3	5	2	1.28200	73.863	2.0

74	3	1	4	1.27600	74.268	3.0
75	0	5	3	1.27600	74.268	3.0
76	0	6	2	1.26410	75.087	2.0
77	1	5	3	1.26000	75.374	2.0
78	4	3	3	1.25660	75.614	1.0
79	5	4	1	1.24990	76.091	1.0
80	3	6	0	1.24140	76.707	1.0
81	5	1	3	1.23270	77.348	1.0
82	1	7	2	1.10070	88.826	1.0
83	3	7	0	1.09610	89.298	1.0
84	2	6	3	1.09610	89.298	1.0

Stick Pattern

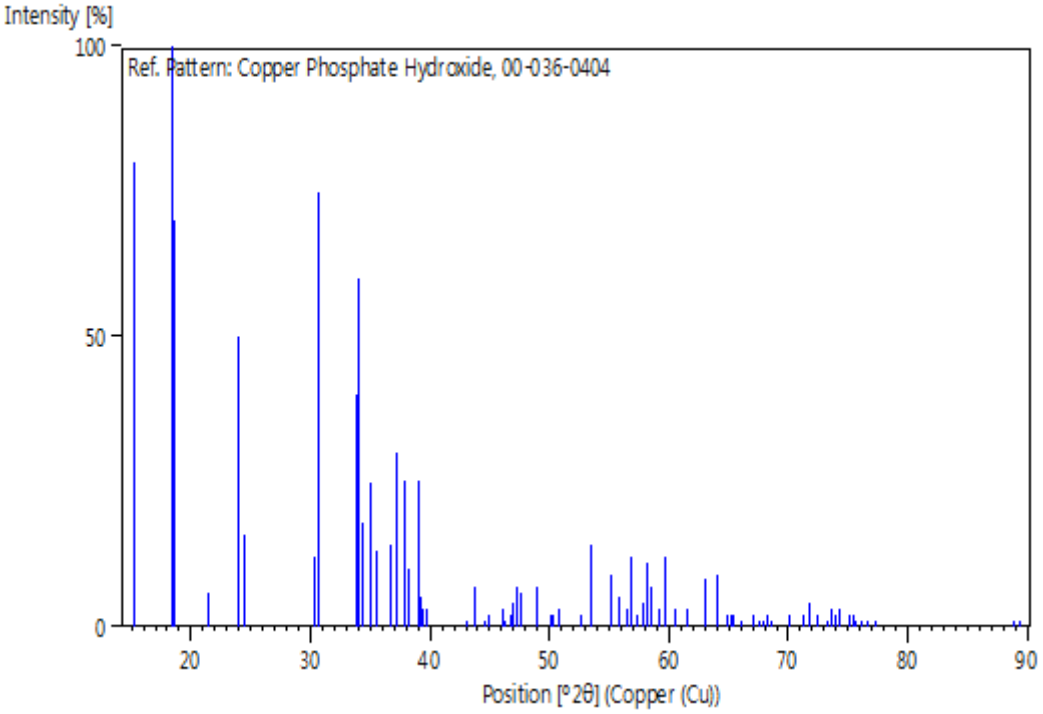

TiO_2 (anatase) JCDD file

Name and formula

Reference code:	01-086-1156
Mineral name:	Anatase, syn
Compound name:	Titanium Oxide
PDF index name:	Titanium Oxide
Empirical formula:	$O_2Ti_{0.784}$
Chemical formula:	$Ti_{0.784}O_2$

Crystallographic parameters

Crystal system:	Tetragonal
Space group:	I41/amd
Space group number:	141

a (Å):	3.7800
b (Å):	3.7800
c (Å):	9.5100
Alpha (°):	90.0000
Beta (°):	90.0000
Gamma (°):	90.0000
Volume of cell (10^6 pm^3):	135.88
Z:	4.00
RIR:	3.93

Status, subfiles and quality

Status:	Alternate Pattern
Subfiles:	Alloy, metal or intermetalic, Inorganic, Mineral, Mineral - Mineral, Mineral - Synthetic
Quality:	Indexed (I)

Comments

ANX:	N3O8
ICSD collection code:	82082
Creation Date:	01/09/1999
Modification Date:	01/09/2011
Cross-References:	ICSD:82082
ANX:	N3O8
Analysis:	O2 Ti0.784
Formula from original source:	Ti0.784 O2
ICSD Collection Code:	82082
Calculated Pattern Original Remarks:	Minority phase (11%) in mixture with rutile from gel dried at 343 K for 24h and annealed at 673 K for 12h in air. Nanophase with 21 nm grain size (8 nm before heating)
Minor Warning:	No R factors reported/abstracted
Wyckoff Sequence:	e a(I41/AMDZ)
Unit Cell Data Source:	Powder Diffraction.

References

Primary reference: *Calculated from ICSD using POWD-12++*, (1997)
Structure:Sanchez, E., Lopez, T., Gomez, R., Bokhimi, Morales, A., Novaro, O., *J. Solid State Chem.*, **122**, 309, (1996)

Peak list

No.	h	k	l	d [Å]	2θ [°]	I [%]
1	1	0	1	3.51269	25.335	100.0
2	1	0	3	2.42893	36.980	2.3
3	0	0	4	2.37750	37.809	17.0
4	1	1	2	2.32998	38.611	3.0
5	2	0	0	1.89000	48.104	26.9
6	1	0	5	1.69904	53.921	17.0
7	2	1	1	1.66438	55.138	14.7
8	2	1	3	1.49163	62.184	1.2
9	2	0	4	1.47948	62.752	9.6
10	1	1	6	1.36332	68.807	5.1
11	2	2	0	1.33643	70.393	5.3
12	1	0	7	1.27850	74.099	0.2
13	2	1	5	1.26354	75.126	8.0
14	3	0	1	1.24908	76.150	1.9
15	0	0	8	1.18875	80.781	0.1
16	3	0	3	1.17090	82.275	0.3
17	2	2	4	1.16499	82.784	3.1
18	3	1	2	1.15927	83.283	0.8
19	2	1	7	1.05897	93.338	0.2
20	3	0	5	1.05042	94.332	1.7
21	3	2	1	1.04207	95.327	1.7
22	1	0	9	1.01765	98.390	0.9
23	2	0	8	1.00626	99.904	0.3

24	3	2	3	0.99536	101.409	0.3
25	3	1	6	0.95436	107.634	2.2
26	4	0	0	0.94500	109.201	1.1
27	3	0	7	0.92384	112.983	0.1
28	3	2	5	0.91814	114.064	2.1
29	4	1	1	0.91255	115.154	1.1
30	1	1	10	0.89598	118.573	3.2
31	2	1	9	0.89598	118.573	3.2
32	2	2	8	0.88822	120.280	0.3
33	4	1	3	0.88069	122.007	0.2
34	4	0	4	0.87817	122.604	1.1
35	3	3	2	0.87572	123.194	0.2
36	4	2	0	0.84523	131.384	1.7
37	1	0	11	0.84278	132.127	0.4
38	3	1	8	0.84278	132.127	0.4
39	3	2	7	0.82999	136.276	0.2
40	4	1	5	0.82585	137.729	1.7
41	3	0	9	0.80964	144.130	0.5

Stick Pattern

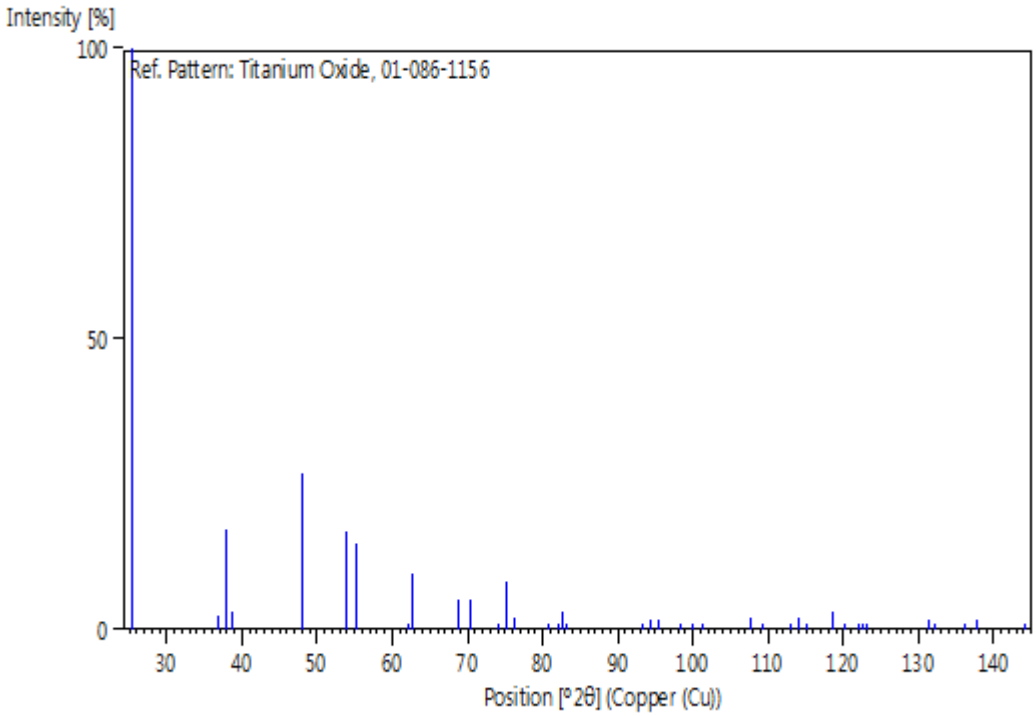

TiO_2 (rutile) JCDD file

Name and formula

Reference code:	00-021-1276
Mineral name:	Rutile, syn
Compound name:	Titanium Oxide
Common name:	titania
PDF index name:	Titanium Oxide
Empirical formula:	O_2Ti
Chemical formula:	TiO_2
Mineral classification:	Rutile (Supergroup), 1Q (Group)

Crystallographic parameters

Crystal system:	Tetragonal
Space group:	P42/mnm
Space group number:	136
a (Å):	4.5933
b (Å):	4.5933
c (Å):	2.9592
Alpha (°):	90.0000
Beta (°):	90.0000
Gamma (°):	90.0000
Calculated density (g/cm^3):	4.25
Measured density (g/cm^3):	4.23
Volume of cell (10^6 pm^3):	62.43
Z:	2.00
RIR:	3.40

Subfiles and quality

Subfiles:	Alloy, metal or intermetalic, Common Phase, Educational pattern, Excipient, Forensic, Inorganic, Mineral, Mineral - Mineral, Mineral - Synthetic, NBS pattern, Pharmaceutical, Pigment/Dye
Quality:	Star (S)

Comments

Color:	White
Creation Date:	01/09/1971
Additional Patterns:	Validated by calculated pattern
Analysis:	No impurity over 0.001%
Color:	White
General Comments:	Pattern reviewed by Syvinski, W., McCarthy, G., North Dakota State Univ, Fargo, North Dakota, USA, ICDD Grant-in-Aid (1990). Agrees well with experimental and calculated patterns. Additional weak reflections (indicated by brackets) were observed. Naturally occurring material may be reddish brown
Optical Data Specimen location:	Optical data on specimen from Dana`s System of Mineralogy, 7th Ed., I 555
Polymorphism/Phase Transition:	Two other polymorphs, anatase (tetragonal) and brookite (orthorhombic), converted to rutile on heating above 700 C
Reflectance:	Opaque mineral optical data on specimen from Sweden: R3R%=20.3, Disp.=Std. Sample Source or Locality: Sample obtained from National Lead Co., South Amboy, New Jersey, USA. Temperature of Data Collection: Pattern taken at 298 K. Vickers Hardness Number: VHN100=1132-1187. Unit Cell Data Source: Powder Diffraction.

References

Primary reference: *Natl. Bur. Stand. (U. S.) Monogr. 25*, **7**, 83, (1969)
Optical data: *Dana's System of Mineralogy, 7th Ed.*, **I**, 575

Peak list

No.	h	k	l	d [Å]	2θ [°]	I [%]
1	1	1	0	3.24700	27.447	100.0
2	1	0	1	2.48700	36.086	50.0
3	2	0	0	2.29700	39.188	8.0
4	1	1	1	2.18800	41.226	25.0
5	2	1	0	2.05400	44.052	10.0
6	2	1	1	1.68740	54.323	60.0
7	2	2	0	1.62370	56.642	20.0
8	0	0	2	1.47970	62.742	10.0
9	3	1	0	1.45280	64.040	10.0
10	2	2	1	1.42430	65.480	2.0
11	3	0	1	1.35980	69.010	20.0
12	1	1	2	1.34650	69.790	12.0

13	3	1	1	1.30410	72.410	2.0
14	3	2	0	1.27390	74.411	1.0
15	2	0	2	1.24410	76.510	4.0
16	2	1	2	1.20060	79.822	2.0
17	3	2	1	1.17020	82.335	6.0
18	4	0	0	1.14830	84.260	4.0
19	4	1	0	1.11430	87.464	2.0
20	2	2	2	1.09360	89.557	8.0
21	3	3	0	1.08270	90.708	4.0
22	4	1	1	1.04250	95.275	6.0
23	3	1	2	1.03640	96.017	6.0
24	4	2	0	1.02710	97.176	4.0
25	3	3	1	1.01670	98.514	1.0
26	4	2	1	0.97030	105.099	2.0
27	1	0	3	0.96440	106.019	2.0
28	1	1	3	0.94380	109.406	2.0
29	4	0	2	0.90720	116.227	4.0
30	5	1	0	0.90090	117.527	4.0
31	2	1	3	0.88920	120.059	8.0
32	4	3	1	0.87740	122.788	8.0
33	3	3	2	0.87380	123.660	8.0
34	4	2	2	0.84370	131.847	6.0
35	3	0	3	0.82920	136.549	8.0
36	5	2	1	0.81960	140.052	12.0
37	4	4	0	0.81200	143.116	2.0
38	5	3	0	0.78770	155.869	2.0

Stick Pattern

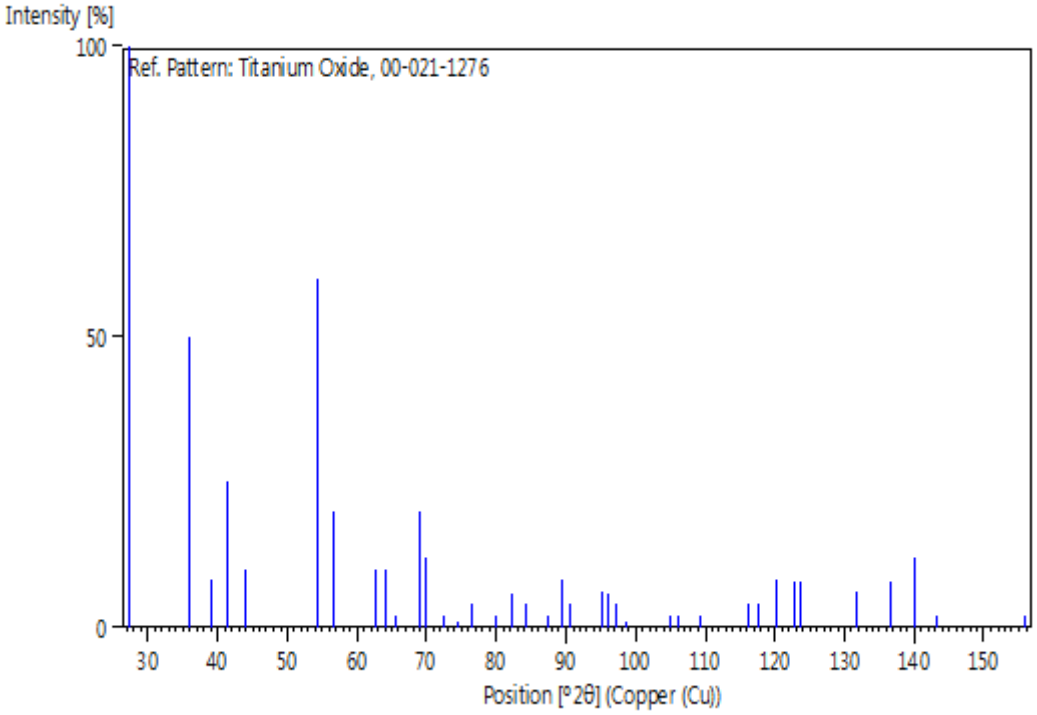

APPENDIX 3

In this appendix IR spectra for the altered IL-assisted method samples and various-ILs-method samples are displayed.

Alternative IL-assisted methods

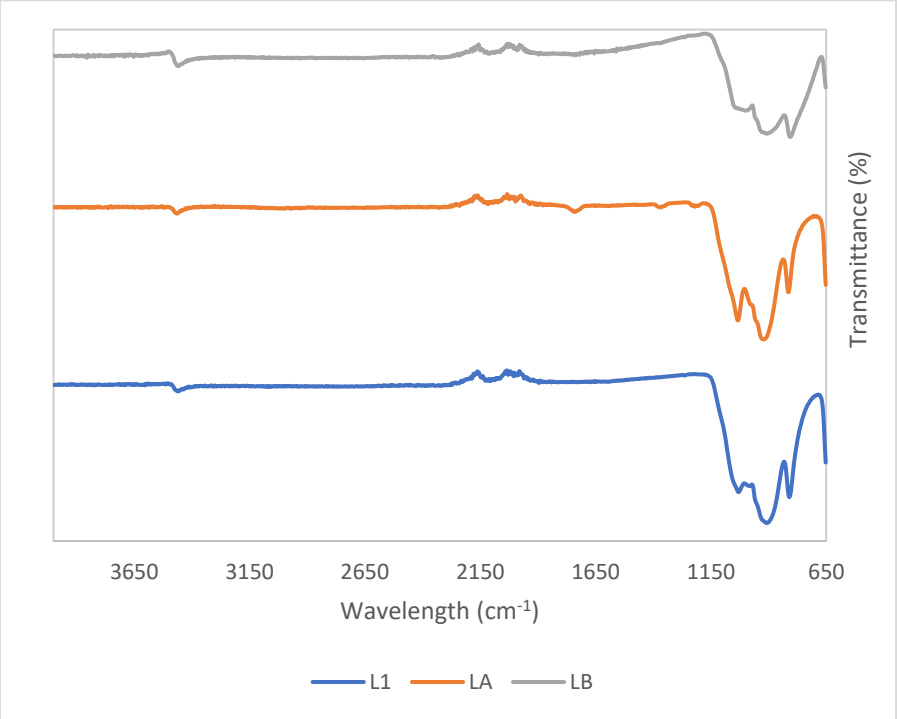

Figure 16. IR spectra of L1, LA and LB.

IR data in the figure above allows to successfully identify the three samples with libethenite, as all peaks and bands match with previous samples and literature.

Synthesis of Cu2(OH)PO4 with various ILs

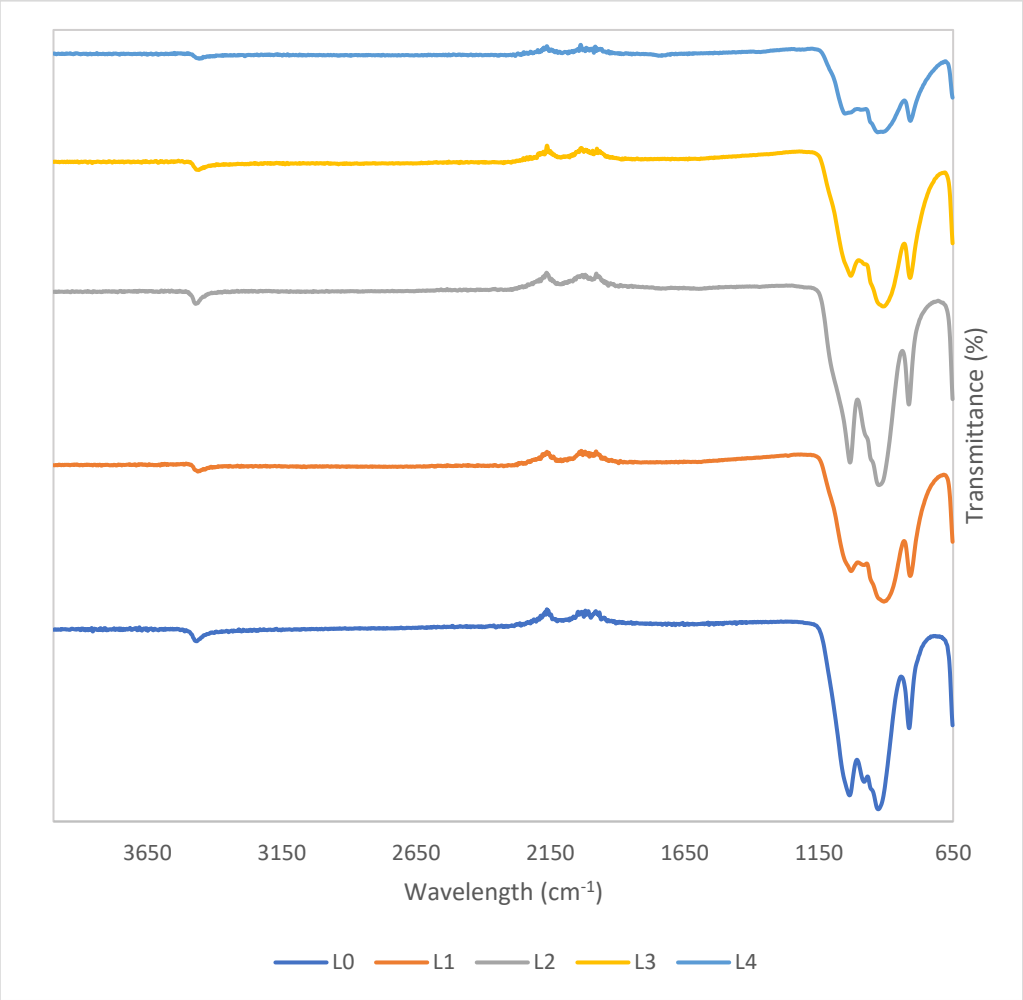

Figure 17. IR spectra for L0, L1, L2, L3 and L4.

Alike samples L1, LA and LB, L0, L2, L3 and L4 could correctly identify as libethenite because of their IR matching with previous samples and literature.

APPENDIX 4

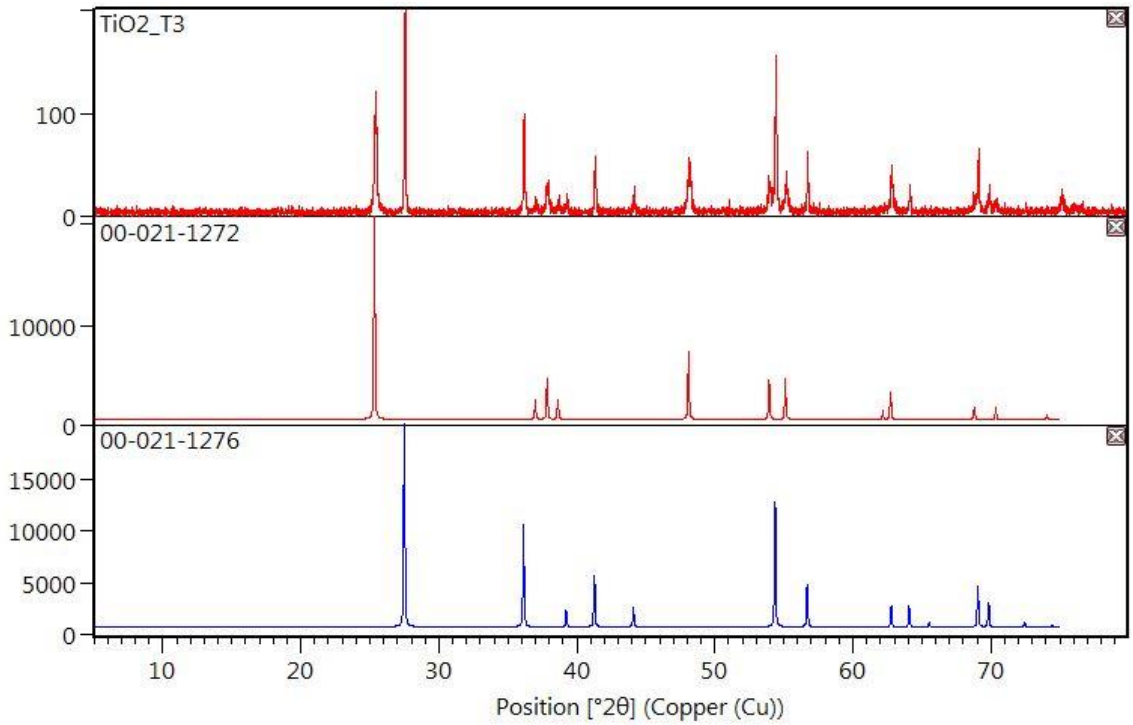

Figure 18.Diffractograms of sample T3 and simulations of JCDD diffraction patterns for anatase and rutile.

Figure 18 displays diffraction simulations for pure anatase and rutile TiO_2 phases and the data from sample T3. This makes obvious that T3 is a mixture of both phases, as it happens less importantly with T2 and T4.